

# Dispersion-managed soliton interactions in optical fibers

T. Yu, E. A. Golovchenko, A. N. Pilipetskii, and C. R. Menyuk

Department of Computer Sciences and Electrical Engineering, University of Maryland Baltimore County, Baltimore, Maryland 21250

Received February 11, 1997

We simulated dispersion-managed soliton propagation and interaction in optical fibers. The energy-enhancement factor, together with the time–bandwidth product and the stretching factor, were calculated as a function of the difference in absolute values of accumulated dispersion in the fiber spans. The interaction strength of the dispersion-managed solitons was found to depend on the stretching factor. When this factor is less than 1.5, the interaction is weaker than for ideal solitons. When it is more than 1.5, there is a strong interaction between the pulses, which constrains the energy enhancement for practical applications. © 1997 Optical Society of America

The recent interest<sup>1,2</sup> in dispersion-managed solitons has been stimulated by the possibility of decreasing the path-averaged dispersion of the transmission line, thus reducing the timing jitter. Computer simulations<sup>3,4</sup> and experiments<sup>5</sup> have shown that stable pulses in a fiber with dispersion maps that have large deviations of the local dispersion from the average have enhanced energy relative to solitons in a fiber with uniform dispersion that is equal to the path-averaged dispersion of the map. Solitons in the dispersion map are analogous to stretched pulses in mode-locked fiber lasers.<sup>6</sup> In this Letter we present a computer study of pulse propagation and interaction in a dispersion map consisting of two spans of normal- and anomalous-dispersion fiber with a path-averaged anomalous dispersion  $\langle\beta\rangle = |\beta_1 L_1 + \beta_2 L_2|/L_m$ , where  $L_m = L_1 + L_2$  is the map length. We modeled the pulse evolution in the dispersion-managed fibers, using the nonlinear Schrödinger equation, with the dispersion coefficient  $\beta$  changing periodically along the propagation distance and taking the values of  $\beta_1$  in the positive group-velocity dispersion span of the map and  $\beta_2$  in the negative group-velocity dispersion span of the map.

Keeping  $\langle\beta\rangle$  and the FWHM pulse duration constant and varying  $\Delta\beta = |\beta_1 - \beta_2|$ , the dispersion difference in the spans, we found the shapes of the stable dispersion-managed solitons by trial and error. Here we define the stable pulses as dispersion-managed solitons to emphasize that the temporal and spectral shape of these pulses repeats itself each map period. However, inside the map these pulses undergo periodic expansion and compression.<sup>3</sup> Typically, the values of the local dispersion in each of the spans that constitute the map are much larger than the path-averaged dispersion. Thus the pulse behavior inside each span is dominated by linear dispersion, whereas the much weaker nonlinearity supports the pulse on average. Consequently, the effective nonlinearity for the dispersion-managed solitons is smaller than that for fundamental solitons in uniform-dispersion fibers, resulting in larger energy for single-soliton propagation in the map. For the dispersion-managed solitons, we then determined the energy-enhancement factor relative to the energy of fundamental solitons in uniform-dispersion fibers with the same values of

the average dispersion, the time–bandwidth product  $\Delta\tau\Delta\nu$ , and the maximum stretching factor of a dispersion-managed soliton inside the map cycle. The dispersion map consists of alternating positive- and negative-dispersion spans with lengths  $L_1$  and  $L_2$ . We investigated two maps, one with  $L_1 = L_2$  and another with the same total map length  $L_m$  but with  $L_1 = 9L_2$ . We tried different dispersion-map arrangements for an injected pulse whose initial phase is uniform (chirp free). Stable dispersion-managed solitons form only if the chirp-free pulse is injected into the middle of the negative- or positive-dispersion span. By contrast, initially chirped pulses can be launched at different points on the map to form dispersion-managed solitons.<sup>7</sup> Having obtained stable pulse shapes, we relaunched these pulses into the dispersion-managed fiber to make sure that the amount of dispersive waves generated owing to the nonsoliton components was negligible.

Figure 1 shows the dependence on  $\gamma = 2(\beta_1 L_1 - \beta_2 L_2)/\tau_0^2$  of the energy-enhancement factor, the time–bandwidth product  $\Delta\tau\Delta\nu$ , and the stretching factor, where  $\beta_1$  is the dispersion value in the span of length

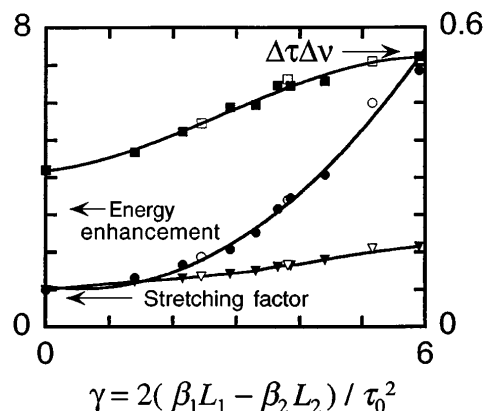


Fig. 1. Energy-enhancement factor (circles), stretching factor (triangles), and time–bandwidth product (squares) versus  $\gamma = 2(\beta_1 L_1 - \beta_2 L_2)/\tau_0^2$ . The filled shapes show the data for a map with equal spans  $L_1 = L_2 = L_m/2$ , and the open shapes correspond to  $L_1 = 9L_2$ . The energy-enhancement factor is the pulse energy normalized to the energy of a fundamental soliton.

$L_1, \beta_2$  is the dispersion value in the span of length  $L_2$ , and  $\tau_0$  is the pulse duration (FWHM). The simulations showed that dispersion-managed soliton parameters are the same for equal values of the parameter  $\gamma$  for both the map with  $L_1 = L_2$  and the map with  $L_1 = 9L_2$ . Thus the parameters of the dispersion-managed solitons depend only on the difference of the accumulated dispersion in each of the map spans, and they are not sensitive to the details of the map itself. As  $\gamma$  increases, the soliton shape evolves from a hyperbolic secant with  $\Delta\tau\Delta\nu = 0.315$  to a Gaussian<sup>3</sup> with  $\Delta\tau\Delta\nu = 0.441$  and into a pulse shape with a spectrum that is nearly square at the top with  $\Delta\tau\Delta\nu = 0.6$ . The time-bandwidth product saturates near  $\Delta\tau\Delta\nu = 0.6$ . Figure 1 shows that the energy-enhancement factor has a nearly quadratic dependence on the parameter  $\gamma$ . In our simulations we obtained dispersion-managed solitons with an energy-enhancement factor as great as 24. Figure 2 shows the pulse shape and the spectrum for  $\gamma = 18.3$  and  $\Delta\tau\Delta\nu = 0.6$ .

For the dispersion-managed solitons that we found, we examined the pulse interaction numerically. For values of as much as  $\gamma = 3.3$ , as shown in Fig. 3, we found that the interaction length—the length over which each soliton retains an independent identity—increases with  $\gamma$ . Moreover, out-of-phase, dispersion-managed solitons repel, as is the case for ideal solitons. Beyond  $\gamma = 3.3$ , corresponding to a stretching factor of 1.5, we found that the interaction length decreases with  $\gamma$  and, moreover, that dispersion-managed solitons attract regardless of the initial phase. The maximum interaction length is obtained with an energy enhancement of  $\sim 2.5$  and a stretching factor of 1.5, and then it rapidly decreases with an increase of the energy enhancement. The maximum interaction length occurs for nearly Gaussian pulses because the tails of the pulses are diminished in comparison with those of fundamental solitons, and the interaction is always attractive at large  $\gamma$  because the large local dispersion tends to average out the phase-dependent contribution. In other words, in the process of interaction a second soliton acts upon the first, whose field we designate  $u_s$ , as a perturbation  $u_p$ . The nonlinear perturbation to the first soliton field owing to the interaction contains terms proportional to  $|u_s|^2 u_p$  and  $|u_p|^2 u_s$ . The strength of the leading-order perturbation  $|u_s|^2 u_p$  depends on the phase of the perturbing field, and the strength of the higher-order perturbation  $|u_p|^2 u_s$  does not. For ideal solitons,  $|u_s|^2 u_p \gg |u_p|^2 u_s$ , and the interaction is phase dependent. When the shapes of the dispersion-managed solitons are transformed from hyperbolic secant to Gaussian with an increase of  $\gamma$ , the pulse tails diminish, thus reducing the interaction strength, while the interaction remains phase dependent. With a further increase of  $\gamma$ , the pulse tails start to overlap significantly owing to the pulse stretching inside the map and thus increase the interaction strength. On the other hand, the phase in the pulse tails is rapidly changing along the propagation distance owing to the strong local dispersion. Thus

the phase-dependent term  $|u_s|^2 u_p$  averages out, and the interaction is governed by the phase-independent term  $|u_p|^2 u_s$ . For the same reason, the interaction of orthogonally polarized pulses at a high enhancement factor and a large stretching degree becomes almost as strong as for copolarized pulses. We verified this point with additional simulations based on the Manakov equations. We also note that the intensity of the dispersive waves in our calculations was  $\sim 8$  orders of magnitude smaller than the pulse intensity, so the interaction between stable pulses was not induced by the dispersive waves.

An example of the dispersion-managed soliton interaction at  $\gamma = 3.65$  is shown in Fig. 4. Note that the interaction of the dispersion-managed solitons is dramatically different from that of fundamental solitons in uniform-dispersion fibers. Figure 4(a) shows the

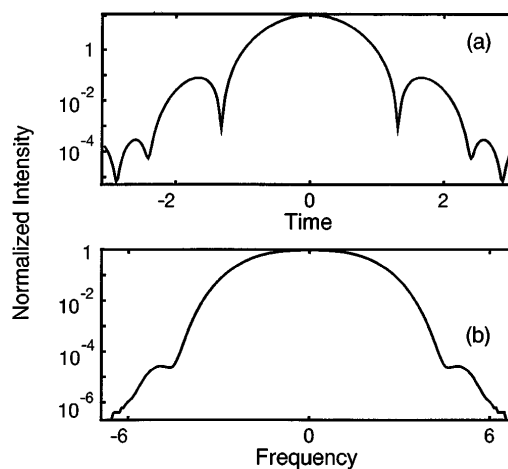


Fig. 2. Intensity and spectrum of a dispersion-managed soliton at  $\gamma = 18.3$  as shown on a logarithmic scale. The time scale is normalized to the pulse FWHM, and the frequency is shown in the soliton units  $(\omega - \omega_0)\tau_0/1.76$ . The time-domain intensity is normalized to the peak intensity of a fundamental soliton at the same average dispersion and pulse duration. The frequency-domain intensity is normalized to the peak intensity.

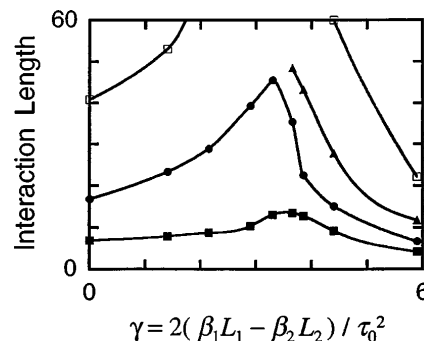


Fig. 3. Dependence of the dispersion-managed soliton interaction length on the parameter  $\gamma$ . The filled squares correspond to the initial pulse separation  $3\tau_0$ , the circles correspond to  $4\tau_0$ , and the open squares correspond to  $5\tau_0$ . The triangles show the interaction length for pulses separated by  $4\tau_0$  that have an initial  $\pi$ -phase difference. The interaction length is normalized to the fundamental soliton period.

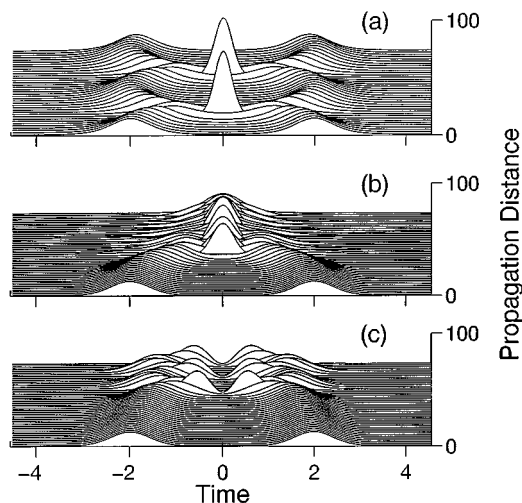


Fig. 4. Interaction of (a) two in-phase fundamental solitons, (b) two in-phase dispersion-managed solitons, and (c) two opposite-phase dispersion-managed solitons for  $\gamma = 3.65$ . The propagation distance is normalized to the fundamental soliton period.

interaction of two fundamental solitons that are initially in phase. In contrast with fundamental solitons that interact periodically, re-emerging undistorted after interaction, the dispersion-managed solitons become closely bound after the first interaction, as shown in Fig. 4(b). These solitons attract each other when  $\gamma > 3.3$ , corresponding to  $\Delta\tau\Delta\nu > 0.45$  and a stretching factor  $> 1.5$  regardless of the initial phase, as shown in Fig. 4(c).

In conclusion, we have studied the interaction of dispersion-managed solitons, and we have shown that there is an optimal energy-enhancement factor beyond which the mutual soliton interaction grows stronger. The shape of the dispersion-managed soliton changes from hyperbolic secant, to Gaussian, to flat top as the enhancement factor grows, and the optimal point corresponds to a nearly Gaussian shape. These results suggest that there is a practical limit to the enhancement factor owing to the mutual interaction.

This research was supported by the National Science Foundation, the U.S. Department of Energy, and the Advanced Research Projects Agency through the U.S. Air Force Office of Scientific Research.

## References

1. M. Suzuki, I. Morita, S. Yamamoto, N. Edagawa, H. Taga, and S. Akiba, *Electron. Lett.* **23**, 2027 (1995).
2. M. Nakazawa and H. Kubota, *Electron. Lett.* **31**, 216 (1995).
3. N. J. Smith, F. M. Knox, N. J. Doran, K. J. Blow, and I. Bennion, *Electron. Lett.* **32**, 54 (1996).
4. E. A. Golovchenko, J. M. Jacob, A. N. Pilipetskii, C. R. Menyuk, and G. M. Carter, *Opt. Lett.* **22**, 289 (1997).
5. J. M. Jacob, E. A. Golovchenko, A. N. Pilipetskii, G. M. Carter, and C. R. Menyuk, *IEEE Photon. Technol. Lett.* **9**, 130 (1997).
6. H. A. Haus, K. Tamura, L. E. Nelson, and E. P. Ippen, *IEEE J. Quantum Electron.* **31**, 591 (1995).
7. N. J. Smith, N. J. Doran, F. M. Knox, and W. Forysiak, *Opt. Lett.* **21**, 1981 (1996).